

Effects of spin-orbit interaction and electron correlations in strontium titanate

Sergei Urazhdin, Ekram Towsif, and Alexander Mitrofanov
Department of Physics, Emory University, Atlanta, GA, USA.

We show that the bottom of the conduction band in SrTiO₃ is formed by the Kramers doublet of states involving a superposition of all three t_{2g} orbitals of Ti mixed by the spin-orbit interaction. Analysis of electron correlations based on the Hubbard model shows that Bloch states derived from this doublet are unstable with respect to the formation of pseudo-spin singlet ground state. These findings may be relevant to both superconductivity and high electron mobility in SrTiO₃ heterostructures.

I. INTRODUCTION

Strontium titanate SrTiO₃ (STO) exhibits unique and puzzling electronic and structural properties that have motivated its extensive studies over the last 50 years [1–4]. The dielectric constant of STO is anomalously large and almost diverges at low temperature without the onset of ferroelectricity, in a manner consistent with quantum paraelectricity [5]. Ferroelectricity in STO can be stabilized by strain or interfacial effects in thin films [6, 7].

Electron-doped STO also exhibits superconductivity (sc) at record-low carrier concentration $n \approx 10^{17} \text{ cm}^{-3}$, corresponding to the Fermi energy of only about 1 meV [5, 8]. Experiments suggest s-wave symmetry of the sc order parameter [9, 10]. Furthermore, the existence of quantum paraelectricity in STO is conducive of the conventional phonon mechanism of sc. However, sc in STO cannot be explained by the conventional Bardeen-Cooper-Schrieffer (BCS) or Migdal-Eliashberg theories relying on the electron-electron attraction mediated by the retarded lattice response to electron motion [11, 12], since the Fermi energy in STO is comparable to or smaller than the energy of phonons mediating sc [13, 14].

The dome-like dependence of the critical temperature T_c on doping in STO is similar to that of high-temperature superconductors, albeit with a small maximum $T_c = 0.4 \text{ K}$ [15, 16]. Furthermore, tunneling measurements provide evidence for multi-band sc, similar to pnictides and some other unconventional superconductors [17]. A variety of models were developed to explain sc in STO, including long-range electron-phonon interaction [18], soft bosonic modes [19], intervalley phonons [20] and quantum paraelectric fluctuations [21, 22], but its mechanism remains debated. In particular, it remains contentious whether the ferroelectric distortions enhance sc in STO [23] or suppress it [19, 24].

Here, we utilize the tight-binding approximation to analyze the spin and orbital properties of the conduction band in STO. In the limit of negligible spin-orbit coupling (SOC), electrons residing in one of the t_{2g} orbitals of Ti hop only within one of the principal planes. Their orbital state is conserved due to the orbital selectivity of hopping, resulting in the formation of three highly anisotropic conduction sub-bands. The states near the bottom of the conduction band are mixed by SOC into a Kramers doublet with the maximum total angular mo-

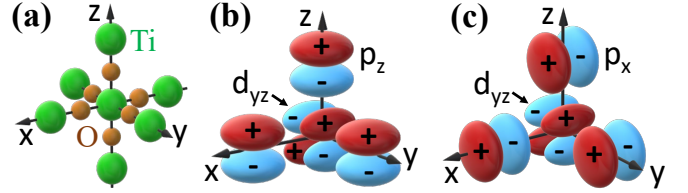


Figure 1. (a) The structural motif dominating the conduction band in STO consists of Ti-O-Ti chains along the principal axes, with octahedral coordination of Ti by oxygen atoms. (b), (c) Schematics of the d_{yz} orbital of Ti and p_z (b), p_x (c) orbitals of nearest-neighbor oxygens on three principal axes. The signs of the orbital lobes are labeled.

mentum $j = 5/2$. We utilize the Hubbard model to show that the Bloch waves formed by these states are unstable at doping levels relevant to sc in STO, resulting in the formation of pseudo-spin singlet ground state. Finally, we present qualitative arguments suggesting that the latter correlations may coexist with sc in STO.

II. CONDUCTION BAND WITHOUT SOC

In this section, we show that in the limit of negligible SOC, the conduction band of STO is characterized by highly anisotropic orbitally-selective transport properties. While the bandstructure of STO has been extensively studied [25–29], we are not aware of prior studies of the relation between the orbital states of electrons and their band properties revealed by our analysis.

STO is a semiconductor that at room temperature has a cubic perovskite structure, with octahedral coordination of Ti formed by six nearest-neighbor oxygens aligned with the principal crystal axes, Fig. 1(a). Antiferrodistortive rotations of the TiO₆ octahedra below 105 K result in small distortions of the octahedral environment of Ti [30]. These distortions may be expected to slightly reduce the orbital selectivity of hopping discussed below, which does not qualitatively change our findings.

The conduction band of STO is dominated by the hopping between t_{2g} orbitals of Ti and p-orbitals of its nearest-neighbor oxygens characterized by the matrix elements $t_{m,m'}^i = \langle d_m | V' | p_{m'}^i \rangle$ [31]. Here, index i enumerates the nearest-neighbor oxygens, d_m is one of the three

t_{2g} orbital wavefunctions of Ti forming a pseudo-vector $(d_{yz}, d_{xz}, d_{xy}) = (d_1, d_2, d_3)$, index m' enumerates oxygen's p-orbitals, and V' is the perturbation of the atomic potential resulting in orbital hybridization. The effects of SOC are analyzed in the next section.

We now show that hopping is described by a single orbitally-selective matrix element. Consider the d_{yz} orbital of Ti and the p_z orbital of the neighboring oxygen on the x-axis, Fig. 1(b). The dependence of the wavefunction d_{yz} on the axial angle θ_x for rotations around the x-axis, measured starting from the y-axis in the positive z-direction, is $\sin(2\theta_x)$. Meanwhile, for the p_z orbital of oxygen on the x-axis, this dependence is $\sin(\theta_x)$. In the cubic phase, the potential V' is axially symmetric. In the cylindrical coordinate system (x, ρ_x, θ_x) aligned with the x-axis, the corresponding matrix element is $t_{1,3}^1 = \int f(x, \rho_x) \sin(\theta_x) \sin(2\theta_x) d\theta_x = 0$, where $f(x, \rho_x)$ is a function of radial and axial coordinates.

This conclusion also follows from the observation that each lobe of the p_z orbital overlaps with both the positive and the negative lobes of the d_{yz} orbital, Fig. 1(b). Hopping between the d_{yz} orbital and the p_z orbital of the oxygen on the z-axis is also prohibited by symmetry. The only symmetry-allowed matrix element involving the d_{yz} orbital, $t_{1,3}^2$, corresponds to hopping to the p_z orbital of nearest-neighbor oxygens on the y axis, since both orbitals are described by the same dependence $\cos(\theta_y)$ on the rotation angle around the y-axis. By the cubic symmetry of STO, the only finite matrix element involving hopping between the d_{yz} orbital of Ti and the p_y orbitals of oxygens is $t_{1,2}^3 = t_{1,3}^2$, which corresponds to hopping along the z-axis. Hopping between d_{yz} and the p_x orbitals is prohibited by symmetry in all directions, Fig. 1(c).

We conclude that an electron in the d_{yz} orbital of Ti can hop only onto the p_z orbital of the two nearest-neighbor oxygens on the y-axis or the p_y orbital of the two nearest-neighbor oxygens on the z-axis. By the same symmetry arguments, it can then only hop from oxygen only onto the d_{yz} orbital of the nearest-neighbor Ti along the corresponding Ti-O-Ti chain [see Fig. 1(b)]. Thus, electrons initially in the d_{yz} orbital propagate only in the yz plane while retaining their orbital state.

Since oxygen merely mediates orbitally-selective hopping between Ti atoms, hereinafter we consider only the state projections on the Ti t_{2g} orbitals. Orbital state-preserving hopping between the d_{yz} orbital of Ti and its four nearest Ti neighbors in the yz plane is described by a single hopping parameter t , which is negative since d_{yz} is antisymmetric with respect to both the y- and the z-axes [see Fig. 1(b)]. By symmetry, hopping of electrons in the d_{xz} and d_{xy} orbitals occurs only within the xz and xy planes, respectively. The corresponding Hubbard Hamiltonian is

$$\hat{H}_{hop} = \sum \epsilon_0 \hat{n}_{\vec{n},m,s} + t(1 - \delta_{l,m}) \hat{c}_{\vec{n}+\vec{l},m,s}^+ \hat{c}_{\vec{n},m,s}, \quad (1)$$

where ϵ_0 is the level energy, $\hat{c}_{\vec{n},m,s}^+$ is the electron creation operator on site \vec{n} in orbital d_m with projection $s = \pm 1/2$

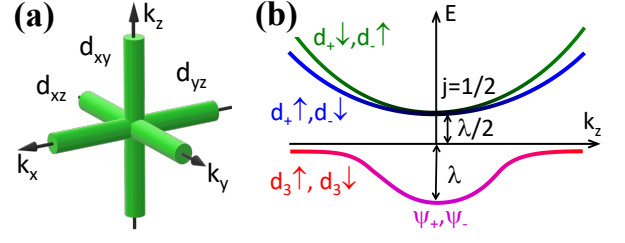


Figure 2. (a) In the limit of negligible SOC, the Fermi surfaces of the sub-bands derived from the orbitals d_m are cylinders spanning the Brillouin zone and aligned with the reciprocal axes. (b) SOC conduction band structure along k_z .

of spin on the z-axis, $\hat{n}_{\vec{n},m,s} = \hat{c}_{\vec{n},m,s}^+ \hat{c}_{\vec{n},m,s}$, \vec{l} is a unit vector in one of the two directions along the l^{th} principal axis, $\delta_{l,m}$ is the Kronecker symbol.

The single-particle eigenstates derived from the orbitals d_m are Bloch waves

$$\psi_{\vec{k},m,s} = \frac{1}{\sqrt{N}} \sum e^{ia\vec{k}\vec{n}} \hat{c}_{\vec{n},m,s}^+ |0\rangle = \hat{c}_{\vec{k},m,s}^+ |0\rangle \quad (2)$$

where a is the lattice constant and N is the total number of sites. Their dispersion is

$$E_m(\vec{k}) = \epsilon_0 + 2t \sum_{m'} (1 - \delta_{m,m'}) \cos(k_m a). \quad (3)$$

We choose $\epsilon_0 = -4t$ so that \hat{H}_{hop} is the kinetic energy. In the discussed approximation, the m^{th} sub-band is non-dispersive in the m^{th} direction and is parabolic at small k in the other two directions. The Fermi surface consists of three orbitally-selective cylindrical sub-surfaces aligned with the reciprocal axes and spanning the Brillouin zone, Fig. 2(a).

III. SOC EFFECTS

The atomic SOC Hamiltonian is $\hat{H}_{SO} = -\lambda \vec{L} \cdot \vec{s}$, where $\lambda \approx 18$ meV for STO, \vec{L} and \vec{s} are the orbital and the spin angular momenta in units of Planck constant. The projection of this Hamiltonian on the t_{2g} subspace is

$$\hat{H}_{SO} = i \frac{\lambda}{2} \sum e_{m_1 m_2 m_3} \sigma_{ss'}^{m_1} \hat{c}_{\vec{k},m_2,s}^+ \hat{c}_{\vec{k},m_3,s'}, \quad (4)$$

where $e_{m_1 m_2 m_3}$ is the Levi-Civita symbol σ^m and is the m^{th} Pauli matrix.

A general solution for $\hat{H} = \hat{H}_{hop} + \hat{H}_{SO}$ at arbitrary \vec{k} is precluded by the anisotropy of hopping. For \vec{k} along k_z , the d_1 and d_2 sub-bands are degenerate, and split from the d_3 sub-band by $\Delta E \approx ta^2 k^2$. According to the perturbation theory, their mixing with the d_3 sub-band is negligible at $k \gg a^{-1} \sqrt{\lambda/t}$. The eigenstates of \hat{H} on the d_1, d_2 orbital subspace are Bloch waves with the atomic orbital structure $d_{\pm} = (d_1 \pm id_2)/\sqrt{2}$ characterized by

definite orbital moment projections $M = \pm 1$ on the z -axis, resulting in the splitting of the d_1 , d_2 band into a two-fold degenerate $j = 1/2$ sub-band $d_+ \uparrow$, $d_- \downarrow$, and $j = 3/2$ sub-band $d_- \uparrow$, $d_+ \downarrow$ split by λ . Here, the up/down arrows denote the spin direction.

At $k = 0$, the kinetic energy vanishes and \hat{H} can be diagonalized. The ground state is split by SOC into a Kramers doublet with the atomic spin-orbital structure

$$\begin{aligned}\psi_+ &= (\sqrt{2}d_+ \uparrow - d_3 \downarrow)/\sqrt{3} \\ \psi_- &= (\sqrt{2}d_- \downarrow + d_3 \uparrow)/\sqrt{3}\end{aligned}\quad (5)$$

with $j = 5/2$ and energy $\epsilon_{\pm} = -\lambda$, and a four-fold degenerate state with atomic structure

$$\begin{aligned}\psi_1 &= (\sqrt{2}d_+ \uparrow + 2d_3 \downarrow)/\sqrt{6}, \\ \psi_2 &= (\sqrt{2}d_- \downarrow - 2d_3 \uparrow)/\sqrt{6} \\ \psi_3 &= d_+ \downarrow, \quad \psi_4 = d_- \uparrow,\end{aligned}\quad (6)$$

with $j = 1/2$ and energy $\epsilon_n = \lambda/2$. We note that ψ_{\pm} are ground states of \hat{H}_{SO} on the full space of all five d-orbitals, since they minimize the SO energy. In contrast, the $j = 1/2$ quadruplet are eigenstates of only the projection of \hat{H}_{SO} on the t_{2g} subspace, since only $j = 5/2$ and $j = 3/2$ states are eigenstates of this Hamiltonian on the full space of five d-orbitals.

We use perturbation theory to analyze the effects of hopping [32]. At $k \ll a^{-1}\sqrt{\lambda/t}$, hopping-induced mixing between the lowest-energy doublet ψ_{\pm} , and the $j = 1/2$ quadruplet is negligible. The hopping term is diagonal on the subspace of plane waves

$$\psi_{\vec{k},\sigma}^{(0)} = \frac{1}{\sqrt{N}} \sum e^{i\vec{k}\vec{n}} \hat{c}_{\vec{n},\sigma}^+ |0\rangle = \hat{c}_{\vec{k},\sigma}^+ |0\rangle \quad (7)$$

where $\sigma = \pm$ is pseudo-spin, the operator $\hat{c}_{\vec{n},\sigma}^+$ creates an electron in the state ψ_{σ} on site \vec{n} , and operator $\hat{c}_{\vec{k},\sigma}^+$ creates an electron in the corresponding Bloch state.

The dispersion of the Bloch states Eq. (7) $\epsilon_{\sigma}(k) = [\frac{2}{3}t(ka)^2 - \lambda]$ is isotropic and independent of σ , with effective mass $m^* = 3\hbar^2/4ta^2$. In contrast, the sub-bands derived from the $j = 1/2$ states are anisotropic. For instance, the bands derived from $\psi_{1,2}$ are characterized by the effective mass $m_1 = 3\hbar^2/5ta^2$ along the k_x and k_y axes, and $m_3 = 3\hbar^2/2ta^2$ along the k_z axis.

The degeneracy of the sub-bands derived from ψ_{σ} is protected by a combination of time reversal and spatial inversion symmetries [33]. The latter is preserved by the antiferrodistortive transition but lifted by the ferroelectric distortions at large doping.

Our analysis of SOC bandstructure is consistent with the observation of a quasi-isotropic Fermi surface at light doping [34]. The measured $m^* = 1.6 \times 10^{-30}$ kg allows us to estimate $t = 0.2$ eV. Hopping-induced orbital hybridization resulting in orbital moment quenching is expected to onset around $k_F = a^{-1}\sqrt{\lambda/t}$, where $k_F = \sqrt[3]{3\pi^2 n}$ is the Fermi wave vector, which corresponds

to doping $n \sim 10^{19}$ cm $^{-3}$. At larger doping, hopping results in the emergence of anisotropic bandstructure obtained in Section II in the limit of negligible SOC. The first-order hopping correction to $\psi_{\vec{k},\sigma}^{(0)}$ is

$$\psi_{\vec{k},\sigma}^{(1)} = - \sum_n \frac{\langle \psi_{\vec{k},n}^{(0)} | \hat{H}_{hop} | \psi_{\vec{k},\sigma}^{(0)} \rangle}{\epsilon_n - \epsilon_{\sigma}} \psi_{\vec{k},n}^{(0)}, \quad (8)$$

where $\psi_{\vec{k},n}^{(0)}$ are Bloch states derived from the orbitals ψ_n . For $\sigma = +$, the only finite matrix element is $n = 1$, and for $\sigma = -$ it is $n = 2$. To the lowest order in ka ,

$$\begin{aligned}\langle \psi_{\vec{k},1}^{(0)} | \hat{H}_{hop} | \psi_{\vec{k},+}^{(0)} \rangle &= \langle \psi_{\vec{k},2}^{(0)} | \hat{H}_{hop} | \psi_{\vec{k},-}^{(0)} \rangle \\ &= \frac{ta^2}{3\sqrt{2}} (2k_z^2 - k_x^2 - k_y^2),\end{aligned}\quad (9)$$

and $\epsilon_n - \epsilon_{\sigma} \approx 3\lambda/2$. For $k \gtrsim a^{-1}\sqrt{\lambda/t}$ along k_z , ψ_{σ} are mixed by hopping with other spin-orbital states, evolving at large k into $d_3 \uparrow$, $d_3 \downarrow$ [Fig. 2(b)]. Meanwhile, the $j = 1/2$ quadruplet evolves into two d_{\pm} sub-bands discussed above in the large- k limit. By symmetry, the dependences are similar for other principal directions. *Ab initio* calculations for heavy doping predict a highly anisotropic star-shaped Fermi surface stretched along the principal axes, in agreement with this analysis [28].

IV. FERMI SURFACE INSTABILITY DUE TO ELECTRON-ELECTRON INTERACTION

We analyze the effects of Coulomb interactions between electrons using the Mott-Hund's interaction Hamiltonian [35]

$$\begin{aligned}\hat{H}_{int} &= \sum U \hat{n}_{\vec{n},m,\uparrow} \hat{n}_{\vec{n},m,\downarrow} \\ &+ (U - 2J) \hat{n}_{\vec{n},m,s} \hat{n}_{\vec{n},m',<m,-s} \\ &+ (U - 3J) \hat{n}_{\vec{n},m,s} \hat{n}_{\vec{n},m',<m,s}.\end{aligned}\quad (10)$$

The first term is the Mott's energy of electrons with opposite spins on the same orbital, the other two represent the Hund's energy of electrons on different orbitals, with common notations for the coefficients [36, 37].

As shown in the previous section, the conduction band states are derived from the spin-orbit coupled Kramers doublet ψ_{σ} with orbital composition that is almost independent of k for $n < 10^{19}$ cm $^{-3}$. The interaction Hamiltonian Eq. (10) projected on the states ψ_{σ} with atomic structure Eq. (5) is

$$\hat{H}_{int} = V \sum_{\vec{n}} \hat{c}_{\vec{n},+}^+ \hat{c}_{\vec{n},-}^+ \hat{c}_{\vec{n},-} \hat{c}_{\vec{n},+}, \quad (11)$$

where $V = U - 16J/9 > 0$ and $\hat{c}_{\vec{n},\sigma}$ annihilates electron in the state ψ_{σ} on site \vec{n} . Equation (11) is similar to the Mott's energy, with spin replaced by the pseudo-spin σ .

At $n > 10^{19} \text{ cm}^{-3}$, the orbital composition of the conduction band states exhibits a significant dependence on \vec{k} . Nevertheless, only two pseudo-spin-degenerate subbands are occupied until they become filled at $n = 2/a^3 \sim 10^{22} \text{ cm}^{-3}$. According to the Pauli principle, the form of interaction Eq. (11) is preserved at heavy doping, but the effective interaction becomes wavevector-dependent. For simplicity, we neglect this dependence.

To analyze the effects of interaction, we consider a volume $\Omega = L^3$, where $L = \sqrt[3]{N}a$ is the linear dimension, selected so that it contains just two electrons in the conduction band. The kinetic energy is minimized in the Bloch state with momentum $k = 0$ for both electrons. According to the Pauli principle, they must occupy both states ψ_+ and ψ_- , so the interaction energy is $E_{int} = V$. On the other hand, if the two electrons are localized on different sites, their interaction energy vanishes, but their kinetic energy increases by $4t$. Thus, one may expect that interaction can lead to instability of the Bloch states [38, 39].

In the reciprocal space, the onset of instability is expected to be manifested by finite wavefunction components with the smallest possible nonzero wavevectors $\vec{k}_{\vec{l}} = 2\pi\vec{l}/L$ for one of the two electrons, allowing the electrons to reduce their spatial overlap while minimizing the increase of kinetic energy. Here, \vec{l} is a unit vector along one of the principal axes.

Consider a trial two-electron wavefunction

$$\Psi = (\alpha\hat{c}_{0,+}^+\hat{c}_{0,-}^+ + \beta_+\hat{c}_{0,+}^+\hat{c}_{\vec{k}_{\vec{l}},-}^+ + \beta_-\hat{c}_{0,-}^+\hat{c}_{\vec{k}_{\vec{l}},+}^+)|0\rangle, \quad (12)$$

where $\hat{c}_{\vec{k},\sigma}^+$ creates a Bloch wave derived from ψ_σ , and $|\alpha|^2 + |\beta_+|^2 + |\beta_-|^2 = 1$. The kinetic energy is

$$E_{kin} = \epsilon_1(|\beta_+|^2 + |\beta_-|^2), \quad (13)$$

where $\epsilon_1 = 2\hbar^2\pi^2/m^*L^2$ is the energy of the $\vec{k}_{\vec{l}}$ state relative to the $k = 0$ state.

The interaction energy obtained by transforming Eq. (12) into the coordinate representation is

$$E_{int} = V[1 - 2\text{Re}(\beta_+\beta_-^*)]. \quad (14)$$

Finite β_+ , β_- increase E_{kin} and decrease E_{int} . The latter is minimized in the pseudo-spin singlet state with $\beta_+ = \beta_- = \beta e^{i\phi}$, where β is real and ϕ describes the gauge symmetry of the singlet.

The total energy is

$$E = E_{kin} + E_{int} = V + 2\beta^2(\epsilon_1 - V). \quad (15)$$

Thus, at $V < \epsilon_1$ energy is minimized in the Bloch state with $\alpha = 1$, $\beta = 0$, while at $V > \epsilon_1$ it is minimized in the pure singlet state with $\alpha = 0$, $\beta = 1/\sqrt{2}$, resulting in a quantum transition [19]. The criticality is "soft", in the sense that the ground state (g.s.) becomes massively degenerate with respect to the value of β at $n = n_c$, which is then likely controlled by the parameters such as deviations from the cubic symmetry and defects not included

in our model. Including other wavevectors $\vec{k}_{\vec{l}}$ to the trial wavefunction does not affect the energy of the singlet state, resulting in additional degeneracy of the singlet with respect to the distribution among wavevectors,

$$\Psi_s = \sum_{\vec{l}} \beta_{\vec{l}}(\hat{c}_{0,+}^+\hat{c}_{\vec{k}_{\vec{l}},-}^+ + \hat{c}_{0,-}^+\hat{c}_{\vec{k}_{\vec{l}},+}^+)|0\rangle, \quad (16)$$

limited only by the normalizing condition $\sum |\beta_{\vec{l}}|^2 = 1/2$. These degeneracies may be related to the high sensitivity of the electronic properties of STO to various perturbations such as strain [23, 40].

In our model, the volume $\Omega = L^3$ is determined by the condition that it contains two electrons, or equivalently $L = \sqrt[3]{2/n}$, where n is the electron density. The instability criterion can be then written as

$$n < n_c = \frac{(Vm^*)^{3/2}}{\sqrt{2}\pi^3\hbar^3}. \quad (17)$$

i.e. Bloch states are unstable at sufficiently low doping regardless of the interaction strength. Using the value $m^* = 1.6 \times 10^{-30} \text{ kg}$ [34] and an order-of-magnitude estimate $V \sim 1 \text{ eV}$ based on the typical values of the Mott-Hunds constants [35], we obtain $n_c \sim 10^{21} \text{ cm}^{-3}$, i.e. the Bloch states are expected to be unstable at doping levels relevant to sc in STO.

This analysis does not naturally extend to many-electron states required to describe the correlation effects for a finite Fermi surface. Nevertheless, it suggests that in contrast to Mott's metal-insulator transition driven by a similar mechanism [38, 39], degeneracy of the states Eq. (16) allows them to carry current, i.e. the singlet state is not an insulator but rather a correlated metal. This can be seen from the expression for the band velocity carried by a singlet with a particular value of $\vec{k}_{\vec{l}}$

$$\vec{v}_{\vec{l}} = \frac{1}{\hbar} \frac{d\epsilon(k)}{d\vec{k}} \Big|_{\vec{k}=\vec{k}_{\vec{l}}} = \frac{2^{2/3}\hbar\pi n^{4/3}}{m^*} \vec{l}, \quad (18)$$

which carries a charge current density $\vec{j} = e\vec{v}_{\vec{l}}/Na^3$. In equilibrium, the amplitudes of singlets with opposite $\vec{k}_{\vec{l}}$ are the same, so such a state does not carry a net charge current. Electrical bias is expected to result in re-distribution of singlets among different $\vec{k}_{\vec{l}}$, leading to a net charge current by finite-momentum singlets that does not require a minimum excitation energy.

We now present an alternative derivation of the above results without relying on an *ad hoc* trial wavefunction. We transform \hat{H}_{int} into the momentum representation,

$$\hat{H}_{int} = V \sum_{\vec{k}, \vec{k}', \vec{q}} \hat{c}_{\vec{k}+\vec{q},+}^+ \hat{c}_{\vec{k}'-\vec{q},-}^+ \hat{c}_{\vec{k}',-} \hat{c}_{\vec{k},+}, \quad (19)$$

The first contribution to the interaction energy is provided by the term with $k = k' = q = 0$. The remaining terms include contributions with two zero wavevectors and those where all four wavevectors are finite. The latter are associated with a larger kinetic energy and can be

neglected close to the instability. The remaining terms can be classified into three groups based on which pair of wavevectors have zero values. The first group with the form $\hat{c}_{0,+}^+ \hat{c}_{0,-}^+ \hat{c}_{\vec{q},-} \hat{c}_{-\vec{q},+}$ can be neglected, since it requires that both electrons are in the finite-momentum state. The remaining interaction terms are

$$\begin{aligned} \hat{H}_{int} = & V \hat{n}_{0,+} \hat{n}_{0,-} \\ & + V \sum (\hat{n}_{0,\sigma} \hat{n}_{\vec{k}_l, -\sigma} + \hat{c}_{0,\sigma}^+ \hat{c}_{\vec{k}_l, -\sigma}^+ \hat{c}_{0,-\sigma} \hat{c}_{\vec{k}_l, \sigma}). \end{aligned} \quad (20)$$

The first two terms describe the interaction energy associated with the uncorrelated populations of zero- and finite-momentum states, while the last term describes the effect of correlations between these states that allows electrons to reduce the interaction energy. This equation can be written in an alternative form

$$\hat{H}_{int} = V \hat{n}_{0,+} \hat{n}_{0,-} + V \sum (\hat{n}_{0,\sigma} \hat{n}_{\vec{k}_l, -\sigma} - \hat{b}_l^+ \hat{b}_l), \quad (21)$$

where the operator

$$\hat{b}_l = \hat{c}_{0,+} \hat{c}_{\vec{k}_l, -} + \hat{c}_{0,-} \hat{c}_{\vec{k}_l, +}, \quad (22)$$

annihilates a correlated pair of electrons forming a singlet described by Eq. (16).

The condition that there are two electrons in volume Ω can be written as

$$\hat{n}_{0,+} + \hat{n}_{0,-} + \sum_{\vec{l}, \sigma} \hat{n}_{\vec{k}_l, \sigma} = 2, \quad (23)$$

which allows us to rewrite the first term in Eq. (21) as

$$\hat{n}_{0,+} \hat{n}_{0,-} = \frac{1}{2} (\hat{n}_{0,+} + \hat{n}_{0,-} - \sum_{\vec{l}, \sigma} \hat{n}_{\vec{k}_l, \sigma}). \quad (24)$$

where we have used the identity $\hat{n}_{\vec{k}, \sigma}^2 = \hat{n}_{\vec{k}, \sigma}$ and neglected the terms that require both electrons to be in the finite-wavevector states.

In the absence of magnetism, the electrons are equally distributed between two pseudo-spins,

$$\hat{n}_{0,\sigma} + \sum_{\vec{l}} \hat{n}_{\vec{k}_l, \sigma} = 1. \quad (25)$$

This relation allows us to transform the second term in Eq. (21) into

$$\sum_{\vec{l}} \hat{n}_{0,\sigma} \hat{n}_{\vec{k}_l, -\sigma} = \sum_{\vec{l}} \hat{n}_{\vec{k}_l, -\sigma}, \quad (26)$$

where we have again neglected the term that requires both electrons to be in the finite-wavevector state.

The resulting interaction Hamiltonian is

$$\hat{H}_{int} = \frac{V}{2} \sum (\hat{n}_{0,\sigma} + \hat{n}_{\vec{k}_l, -\sigma} - 2 \hat{b}_l^+ \hat{b}_l). \quad (27)$$

In the mean-field approach, singlet correlations can be described by gauge-symmetric multi-component order parameter

$$\Delta_{\vec{l}} = V \langle \hat{b}_{\vec{l}} \rangle = V \langle \hat{c}_{0,+} \hat{c}_{\vec{k}_l, -} + \hat{c}_{0,-} \hat{c}_{\vec{k}_l, +} \rangle. \quad (28)$$

This order parameter can be utilized to reduce the interaction Hamiltonian Eq. (27) to a quadratic form with respect to fermionic operators, similarly to the mean-field approximation in BCS [11]. This analysis will be presented elsewhere.

Here, we analyze the properties of the Hamiltonian without linearization. The kinetic energy contribution to the Hamiltonian projected on the subspace of states with wavevectors $k = 0$ and \vec{k}_l is

$$\hat{H}_{kin} = \epsilon_1 \sum_{\vec{l}, \sigma} \hat{n}_{\vec{k}_l, \sigma}. \quad (29)$$

The total Hamiltonian can be written as

$$\hat{H} = \hat{H}_{kin} + \hat{H}_{int} = \hat{H}_1 + \hat{H}_2, \quad (30)$$

where \hat{H}_1 and \hat{H}_2 are effective single-particle and two-particle Hamiltonians,

$$\begin{aligned} \hat{H}_1 &= \frac{V}{2} (\hat{n}_{0,+} + \hat{n}_{0,-}) + \sum_{\vec{k}_l, \sigma} (\epsilon_1 + \frac{V}{2}) \hat{n}_{\vec{k}_l, \sigma} \\ \hat{H}_2 &= -V \hat{b}_l^+ \hat{b}_l. \end{aligned} \quad (31)$$

\hat{H}_1 commutes with \hat{H}_2 , and therefore they have a common basis of eigenstates, which are the stationary states of the full Hamiltonian. The two eigenstates of \hat{H}_2 on the space of states of two electrons are the state with no singlets and the state with one singlet arbitrarily distributed over different \vec{l} . The degeneracy arises because singlet energy is independent of \vec{l} . The total energy of the state with one singlet is $E_s = \epsilon_1$. In the state with no singlets, the g.s. of \hat{H}_1 is the Bloch state of two electrons with $k = 0$, and the total energy $E_0 = V$. Thus, at $V > \epsilon_1$ the system experiences a transition from the Bloch g.s. to the singlet g.s. These results are consistent with the analysis based on the correlated wavefunction ansatz Eq. (12) presented above.

The above analysis substantially relied on the fact that the system contains just two electrons. In this approximation, kinetic energy is minimized when one of these vectors is zero, and another is the smallest possible finite wavevector \vec{k}_l . In the more general approach accounting for the finite size of the Fermi surface formed by the Bloch states, one needs to analyze correlations among all possible pairs of wavevectors.

We now argue that the presented mechanism of interaction energy reduction via Mott-like pseudo-spin singlet correlations is relevant to any pair \vec{k}_1, \vec{k}_2 of wavevectors. The wavefunction of the uncorrelated Bloch state

is $\Psi_2 = \hat{c}_{\vec{k}_1, \sigma_1}^+ \hat{c}_{\vec{k}_1, \sigma_2}^+ |0\rangle$, and the corresponding interaction energy is V . The latter vanishes in the singlet state

$$\Psi_s = \frac{1}{\sqrt{2}}(\hat{c}_{\vec{k}_1, +}^+ \hat{c}_{\vec{k}_2, -}^+ + \hat{c}_{\vec{k}_1, -}^+ \hat{c}_{\vec{k}_2, +}^+) |0\rangle. \quad (32)$$

Thus, this correlation mechanism is effective regardless of the specific momenta of electrons involved in the singlet. The vectors must be close to the Fermi surface so that the kinetic energy increase associated with the reduction of the number of available two-electron states from four for Bloch states to two for the singlet state can be compensated by the decrease of their interaction energy. Instead of analyzing the consequences of these correlations for the finite Fermi surface, in the next section we discuss their interplay with BCS correlations.

V. EFFECTIVE MOTT CORRELATIONS VS BCS SUPERCONDUCTIVITY

There is mounting evidence that incipient ferroelectric distortions may be crucial for sc in STO, suggesting an unusual case of phonon-mediated sc [23, 41]. The purpose of this section is to point out a possible interplay between Mott correlations and BCS sc. In the BCS theory, the general form of phonon-mediated electron attraction Hamiltonian is [11]

$$\hat{H}_{int} = \sum_{\vec{k}, \vec{k}', \vec{q}} V'_{\vec{k}, \vec{k}', \vec{q}} \hat{c}_{\vec{k}+\vec{q}, +}^+ \hat{c}_{\vec{k}'-\vec{q}, -}^+ \hat{c}_{\vec{k}', -} \hat{c}_{\vec{k}, +}, \quad (33)$$

with the matrix elements $V'_{\vec{k}, \vec{k}', \vec{q}} < 0$ describing scattering between electrons with initial wavevectors \vec{k} , \vec{k}' via exchange of a virtual phonon with wavevector \vec{q} . This Hamiltonian has the same form as the Mott-Hunds Hamiltonian Eq. (33), except the matrix elements V' are negative and wavevector-dependent. The relation between phonon and electron dispersions dictates that V' sharply peaks at $\vec{q} = 0$, $\vec{k}' = -\vec{k}$, , so that the BCS interaction is often approximated by the diagonal form

$$\hat{H}_{BCS} = \sum_{\vec{k}} V' \hat{c}_{\vec{k}, +}^+ \hat{c}_{-\vec{k}, -}^+ \hat{c}_{-\vec{k}, -} \hat{c}_{\vec{k}, +}. \quad (34)$$

For electrons with opposite momenta at the Fermi surface, the two-electron wavefunction minimizing the BCS energy Eq. (34) is

$$\Psi_s = \beta_1 (\hat{c}_{\vec{k}, +}^+ \hat{c}_{-\vec{k}, -}^+ - \hat{c}_{\vec{k}, -}^+ \hat{c}_{-\vec{k}, +}^+) |0\rangle, \quad (35)$$

which has the same form as Eq. (32), except for the opposite relative signs of the two wavefunction components. This result seems to suggest that BCS correlations are incompatible with the Mott correlations. However, the wavevector dependences of the two Hamiltonians are different, allowing the resulting correlations to coexist.

We assume that $\vec{q} \approx 0$ and \vec{k} , \vec{k}' are on the Fermi surface, since the kinetic energy increase associated with

the correlations must be minimized. Assume that the phonon-mediated attraction is dominant for two electrons with opposite wavevectors [Eq. (34)]. The BCS interaction rapidly decreases with increasing $\vec{k}_0 = \vec{k} + \vec{k}'$, while the Mott-Hunds interaction Eq. (33) is independent of \vec{k}_0 . Consequently, the latter likely becomes dominant at large \vec{k}_0 , resulting in the correlations of the form Eq. (32). Thus, both Mott-Hunds and BCS energies can be accommodated by singlet correlations, with the relative sign of the two components dependent on the relationship between the wavevectors of the two electrons.

VI. CONCLUSIONS

Our central findings are: i) Electron hopping in STO is highly orbitally-selective and anisotropic, ii) At doping levels relevant to sc in STO, the conduction band states are formed by the Kramers doublet that mixes all three t_{2g} orbitals of Ti, and is characterized by the maximal total atomic angular momentum $j = 5/2$, iii) The band states derived from the Kramers doublet are unstable with respect to the Mott interaction, resulting in the formation of finite-momentum pseudo-spin singlets, and iv) Because of the different dependence of the effective Mott correlations and the BCS correlations on the electron wavevectors, the two correlations can coexist.

We now discuss the experimental implications of our results. The predicted highly orbitally- and direction-selective electron hopping may be relevant to the properties of high-mobility electron gas at the STO/LaAlO₃ interfaces [42], where symmetry lowering at the interface is expected to suppress the spin-orbit mixing of the conduction band bottom, resulting in reduced electron scattering due to the selection rules imposed by the orbital moment conservation. This prediction can be experimentally verified by utilizing orbitally-selective electron tunneling into STO, similar to that utilized in MgO-based magnetic tunnel junctions [43]. For instance, for a tunnel junction in the xy plane, an electron injected into the d_{xy} orbital of STO cannot propagate in the direction normal to the tunnel junction, resulting in qualitatively different electronic characteristics than for electron injected into d_{xz} or d_{yz} orbitals. It may be also possible to directly characterize the directional dependence of the orbital state of electrons propagating in a certain direction in STO by utilizing magneto-optical techniques.

The large unquenched orbital moments of the conduction states predicted by our analysis may be manifested by anomalously low g-factor in electron spin resonance (ESR) of the conduction band. To the best of our knowledge, only impurity ESR has been studied so far [44]. This result is remarkable in the context of the commonly-held belief that cubic crystal field effects are sufficient to quench orbital moments of d-bands. Our calculations show that this is not the case for STO. More generally, cubic symmetry lifts the 5-fold degeneracy of d-state manifold, splitting it into the 2-fold orbitally degenerate

e_g manifold with quenched orbital moment and 3-fold orbitally degenerate t_{2g} manifold [32]. The latter is orbitally unquenched, as follows from $d_{\pm} = (d_1 \pm id_2)/\sqrt{2}$.

Our third central result is that the single-electron Bloch states are unstable below the critical density of about 10^{21} cm^{-3} , resulting in the formation of pseudo-spin singlets. This prediction seems to be inconsistent with the Nernst effect measurements that were interpreted in terms of a well-defined Fermi surface at concentrations down to about $5 \times 10^{17} \text{ cm}^{-3}$ [34]. These measurements demonstrated quantum oscillations of the Nernst coefficient as a function of magnetic field, consistent with a well-defined spatial coherence of electronic states. However, such measurements cannot provide information about the nature of the underlying quasiparticles. The proposed singlet state does not break the translational symmetry of the system, preserving its spatial coherence manifested by the Nernst oscillations. Our model suggests that the quasiparticles are singlet electron pairs, which can be tested, for example by the shot noise measurements in tunnel junctions [45]. Another prediction of our model, that the singlet instability is of the first order, should be manifested by an abrupt change of the quasiparticle charge from $2e$ to e at doping level of about 10^{21} cm^{-3} .

Finally, we presented qualitative analysis suggesting that the effective Mott singlet correlations involving spin-orbit-coupled pseudo-spins may coexist with the BCS correlations due to the different dependences on the mo-

menta of the correlated electrons. The effective Mott correlations can be described by a gauge-symmetric mean-field order parameter [see Eq. (28)], raising the possibility that they can directly contribute to sc itself. Analysis of this possibility requires that the model is extended beyond the two-electron approximation utilized in this work. Experimentally, the significance of this possible contribution to sc can be tested by utilizing the isotope effect. In contrast to BCS, isotope substitution should not directly affect sc mediated by the Mott correlations. Prior studies of isotope oxygen substitution yielded results that are essentially opposite of the BCS expectation [24, 46], which was likely influenced by the isotope-induced ferroelectricity [47], suggesting that other isotopes need to be explored.

A possible contribution of effective Mott correlations to sc in STO may provide a connection to high-temperature sc in cuprates envisioned by K.A. Müller [2]. It was recently suggested that sc in cuprates may be associated with the coupling of charge current to superfluidity of Mott's spin singlets mediated by spin-orbit interaction [48]. Analysis presented above indicates that both spin-orbit interaction and singlet correlations play a significant role in STO, suggesting that these mechanisms may be relevant to other unconventional superconductors including pnictides, twisted multilayer graphene, and superconducting ruthenates.

Bandstructure calculations by A.M. and S.U. were supported by the DOE BES Award # DE-SC0018976. Analysis of correlations by S.U. and E.T. were supported by NSF Awards ECCS-1804198 and ECCS-2005786.

-
- [1] J. G. Bednorz and K. A. Müller, *Rev. Mod. Phys.* **60**, 585 (1988).
- [2] 10.3390/condmat5040060.
- [3] M. N. Gastiasoro, J. Ruhman, and R. M. Fernandes, *Annals of Physics* **417**, 168107 (2020), eliashberg theory at 60: Strong-coupling superconductivity and beyond.
- [4] C. Collignon, X. Lin, C. W. Rischau, B. Fauqué, and K. Behnia, *Annual Review of Condensed Matter Physics* **10**, 25 (2019), <https://doi.org/10.1146/annurev-conmatphys-031218-013144>.
- [5] K. A. Müller and H. Burkard, *Phys. Rev. B* **19**, 3593 (1979).
- [6] H. Uwe and T. Sakudo, *Phys. Rev. B* **13**, 271 (1976).
- [7] W. Burke and R. Pressley, *Solid State Communications* **9**, 191 (1971).
- [8] X. Lin, G. Bridoux, A. Gourgout, G. Seyfarth, S. Krämer, M. Nardone, B. Fauqué, and K. Behnia, *Phys. Rev. Lett.* **112**, 207002 (2014).
- [9] X. Lin, C. W. Rischau, C. J. van der Beek, B. Fauqué, and K. Behnia, *Phys. Rev. B* **92**, 174504 (2015).
- [10] X. Lin, A. Gourgout, G. Bridoux, F. m. c. Jomard, A. Pourret, B. Fauqué, D. Aoki, and K. Behnia, *Phys. Rev. B* **90**, 140508 (2014).
- [11] M. Tinkham, *Introduction to superconductivity* (Dover Publications, Mineola, N.Y., 2004).
- [12] F. Marsiglio, *Annals of Physics* **417**, 168102 (2020).
- [13] Y. Takada, *Journal of the Physical Society of Japan* **49**, 1267 (1980), <https://doi.org/10.1143/JPSJ.49.1267>.
- [14] D. A. Kirzhnits, E. G. Maksimov, and D. I. Khomskii, *Journal of Low Temperature Physics* **10**, 79 (1973).
- [15] J. F. Schooley, W. R. Hosler, and M. L. Cohen, *Phys. Rev. Lett.* **12**, 474 (1964).
- [16] C. S. Koonce, M. L. Cohen, J. F. Schooley, W. R. Hosler, and E. R. Pfeiffer, *Phys. Rev.* **163**, 380 (1967).
- [17] G. Binnig, A. Baratoff, H. E. Hoening, and J. G. Bednorz, *Phys. Rev. Lett.* **45**, 1352 (1980).
- [18] V. L. Gurevich, A. I. Larkin, and Y. A. Firsov, *Sov. Phys. - Solid State (Engl. Transl.); (United States)* **4** (1962).
- [19] J. M. Edge, Y. Kedem, U. Aschauer, N. A. Spaldin, and A. V. Balatsky, *Phys. Rev. Lett.* **115**, 247002 (2015).
- [20] P. A. Fleury, J. F. Scott, and J. M. Worlock, *Phys. Rev. Lett.* **21**, 16 (1968).
- [21] C. W. Rischau, X. Lin, C. P. Grams, D. Finck, S. Harms, J. Engelmayr, T. Lorenz, Y. Gallais, B. Fauqué, J. Hemberger, and K. Behnia, *Nature Physics* **13**, 643 (2017).
- [22] S. E. Rowley, L. J. Spalek, R. P. Smith, M. P. M. Dean, M. Itoh, J. F. Scott, G. G. Lonzarich, and S. S. Saxena, *Nature Physics* **10**, 367 (2014).
- [23] K. Ahadi, L. Galletti, Y. Li, S. Salmani-Rezaie, W. Wu, and S. Stemmer, *Science Advances* **5**, 10.1126/sci-

- adv.aaw0120 (2019).
- [24] C. W. Rischau, D. Pulmannová, G. W. Scheerer, A. Stucky, E. Giannini, and D. van der Marel, *Phys. Rev. Research* **4**, 013019 (2022).
- [25] L. F. Mattheiss, *Phys. Rev. B* **6**, 4740 (1972).
- [26] X. Guo, X. Chen, Y. Sun, L. Sun, X. Zhou, and W. Lu, *Physics Letters A* **317**, 501 (2003).
- [27] S. Piskunov, E. Heifets, R. Eglitis, and G. Borstel, *Computational Materials Science* **29**, 165 (2004).
- [28] D. van der Marel, J. L. M. van Mechelen, and I. I. Mazin, *Phys. Rev. B* **84**, 205111 (2011).
- [29] Q. Tao, B. Loret, B. Xu, X. Yang, C. W. Rischau, X. Lin, B. Fauqué, M. J. Verstraete, and K. Behnia, *Phys. Rev. B* **94**, 035111 (2016).
- [30] G. Shirane and Y. Yamada, *Phys. Rev.* **177**, 858 (1969).
- [31] E. Pavarini, *W.M.C. Foulkes in Quantum materials: experiments and theory : lecture notes of the Autumn School on Correlated Electrons 2016 : at Forschungszentrum Julich, 12-16 September 2016* (Forschungszentrum, Zentralbibliothek, Julich, 2016).
- [32] L. D. Landau, *Quantum mechanics: non-relativistic theory* (Pergamon Press, Oxford New York, 1977).
- [33] M. Dresselhaus, G. Dresselhaus, and A. Jorio, *Group Theory: Application to the Physics of Condensed Matter*, SpringerLink: Springer e-Books (Springer Berlin Heidelberg, 2007).
- [34] X. Lin, Z. Zhu, B. Fauque, and K. Behnia, *Phys. Rev. X* **3**, 021002 (2013).
- [35] L. de' Medici and M. Capone, *Springer Series in Solid-State Sciences* , 115–185 (2017).
- [36] G. Chen, Dilemma in strongly correlated materials: Hund's metal vs relativistic mott insulator (2020), arXiv:2012.06752 [cond-mat.str-el].
- [37] L. de' Medici, *Phys. Rev. B* **83**, 205112 (2011).
- [38] N. F. MOTT, *Rev. Mod. Phys.* **40**, 677 (1968).
- [39] P. P. Edwards and M. J. Sienko, *Phys. Rev. B* **17**, 2575 (1978).
- [40] K. Dunnett, A. Narayan, N. A. Spaldin, and A. V. Balatsky, *Phys. Rev. B* **97**, 144506 (2018).
- [41] Y. Kedem, Paradigm shift for quantum paraelectric: softening of longitudinal modes (2020), arXiv:2004.00029 [cond-mat.mtrl-sci].
- [42] A. Ohtomo and H. Y. Hwang, *Nature* **427**, 423 (2004).
- [43] W. H. Butler, *Science and Technology of Advanced Materials* **9**, 014106 (2008).
- [44] M. D. Glinchuk, I. P. Bykov, A. M. Slipenyuk, V. V. Laguta, and L. Jastrabik, *Physics of the Solid State* **43**, 841 (2001).
- [45] P. Zhou, L. Chen, Y. Liu, I. Sochnikov, A. T. Bollinger, M.-G. Han, Y. Zhu, X. He, I. Boz Ovic, and D. Natelson, *Nature* **572**, 493 (2019).
- [46] A. Stucky, G. W. Scheerer, Z. Ren, D. Jaccard, J.-M. Pomirol, C. Barreteau, E. Giannini, and D. van der Marel, *Scientific Reports* **6**, 10.1038/srep37582 (2016).
- [47] M. Itoh, R. Wang, Y. Inaguma, T. Yamaguchi, Y.-J. Shan, and T. Nakamura, *Phys. Rev. Lett.* **82**, 3540 (1999).
- [48] S. Urazhdin, Chiral superconductivity in cuprates mediated by spin-orbit coupling to spinon superfluidity (2022), arXiv:2202.09965 [cond-mat.mtrl-sci].